IMPACT CRATERS AND SURFACE AGE OF THE NORTH POLAR LAYERED DEPOSITS, MARS.
M.E. Landis[1], S. Byrne[1], I.J. Daubar[2], K.E. Herkenhoff[3], C.M. Dundas[3]. [1] Lunar and Planetary Laboratory, University of Arizona, Tucson, AZ USA (mlandis@lpl.arizona.edu) [2]Jet Propulsion Laboratory, Pasadena, CA 91109 [3]US Geological Survey Astrogeology Center, Flagstaff, AZ, 86001.

Introduction: The North Polar Layered Deposits (NPLD) on Mars preserves a stratigraphic record of alternating layers of ice and dust. A first step to dating these layers would be to understand the current surface accumulation rate and or age. However, being able to age date the surface has been complex. Herkenhoff and Plaut [1] assigned an age of less than 120kyr based on the lack of any visible craters within Viking images. Based on two superimposed craters with higher resolution images, Tanaka [2] derived an age of 8.7kyr. Combining Context Camera (CTX) and High Resolution Imaging Science Experiment (HiRISE), Banks et al. [3] cataloged a population of ~100 craters on the surfaces of the NPLD that had recently accumulated. They found, based on the Hartmann production function [4], that the current crater population was in equilibrium with an erasure time scale of 10-20kyr.

Recently, Daubar et al. [5] have measured a new production function for small martian craters based on detections between sets of CTX images. This new production function has allowed us to revisit the surface age of the NPLD. Additional images from HiRISE have also allowed us to refine diameter measurements and build digital terrain models (DTMs) from stereo images to explore the depth-to-diameter (d/D) ratios of the craters. These new data have started to paint a new picture of the recent history of the surface of the NPLD.

Crater diameters: Crater diameters were measured using the ArcMap Crater Helper Tools, available from the United States Geological Survey.

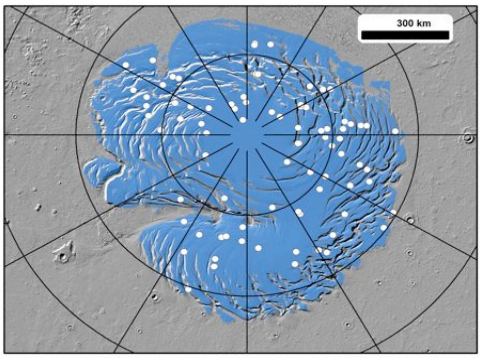

Figure 1: Locations of the craters on the surface of the north pole residual cap, represented by white dots. The blue area is the region of interest from [3] that we adopt as well, with a total area of $7x10^5$ km^2.

Where crater clusters were present, the effective diameter was calculated according to the formula $(\Sigma D^3)^{(1/3)}$ [3,5]. The updated diameter data was on average 2±5m smaller than reported in [3]. The locations of all of these craters are shown in Figure 1.

d/D ratios: Four craters had preexisting DTMs available from the PDS and five additional were constructed as part of this project. The nine total DTMs span a range of visually determined degradation states, from craters with distinct rims and bowl shaped floors to craters that had extensive modification and infilling. These nine craters range in diameter from 35-360m. Figure 2 shows all nine current DTM-derived d/D ratios of NPLD craters.

The range of d/D ratio for the nine craters was 0.197 to 0.02, almost an order of magnitude, with depths measured from surrounding terrain to the floor of the crater as in some cases the crater rims were unevenly degraded. The uncertainty in elevations for the terrain model results are on average ~10cm, determined via the method described in [6]. The pristine d/D ratio for strength-regime craters is ~0.2 (e.g., [7]), including the rim height. These craters represent a range of degradation states from fresh to >90% infilled.

Since there is a range of crater d/D ratios, we interpret this as evidence that these craters are mostly likely from separate impact events rather than a secondary crater field. Therefore, we can use primary crater statistics for analysis of the age of the surface of the NPLD.

Material properties: The NPLD is predominantly

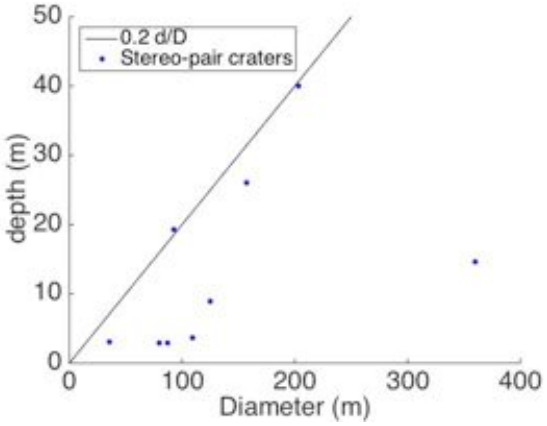

Figure 2: Depth vs. diameter for 9 of the NPLD craters using DTM-derived surroundings-to-floor depths.

pure water ice (e.g., [8]) and therefore will behave differently than bedrock both during the impact and the degradation of the crater.

First, material strengths will produce different diameters of craters. We use pi-group scaling to take into account these differences in material between impacts into dusty regions of Mars in the Daubar et al. [5] production function and impacts into icy material. We modeled the material at the surface of the NPLD as being the density of water ice, the strength and cohesion of soft rock, and the dusty regions as having the regolith parameters in [9]. We took the ratio of the transient diameters in both materials and calculated how different age estimates would be based on strength scaling. We found that at most, we would be over-estimating the age of the surface of the NPLD by a factor of ~2. Further work is needed to refine this scaling analysis.

Second, viscous relaxation is a property of an ice target that does not occur in regolith targets, but that could affect crater diameter sizes. Other work [10] has found that viscous relaxation at these crater diameters would affect depths of these craters more strongly than the diameters. Even then, the effect over the time scales of the resurfacing of the NPLD is small and within the vertical error of the DTM.

Model surface age: Figure 3 shows the differential size-frequency distribution of the impact craters in this study, plotted in red, against several isochrons based on the production functions given in [4] and [5]. The size-frequency distribution of the impact craters on the NPLD is close to the 1kyr isochron of [5], with a best-fit value of ~1.4kyr. Error bars follow the methodology of [11], suited for small number statistics. There is also error (not shown here) associated with the production function determination in [5]. Overall, ages determined are accurate within a factor of two for this population from crater statistics.

Discussion: The closeness of the data to a model age of ~1.4kyr presents two possible scenarios. First, a resurfacing event ~1.4kyr ago could have reset the surface and all visible craters formed afterwards. Second, this may be an equilibrium population with both small and large craters having the same lifetime (~1.4kyr). For shallower craters to persist as long as deeper ones, the accumulation rate within smaller craters must be lower than within the large craters. This is in strong contrast to the conclusions found by [3] using the isochron system of [4]. The isochron system of [4] indicates that the current crater population accumulated over the past 10-15kyr, as small craters have been preferentially infilled. Modeling infilling rates within craters on the NPLD would distinguish between these scenarios. We currently favor the results using the Daubar et al. [5] production function because it is derived from currently observed martian small craters over a temporal baseline more similar to that of the NPLD surface than used by [4].

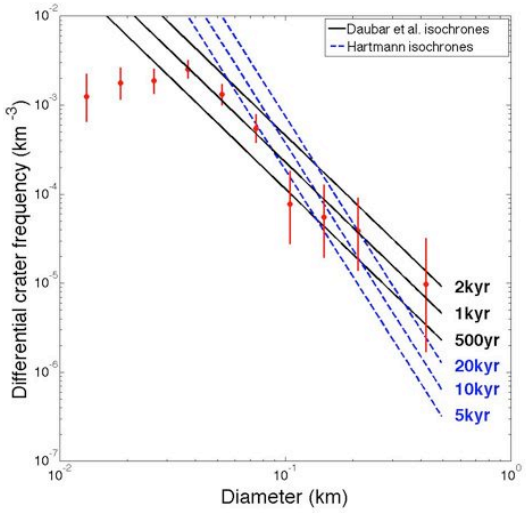

Figure 3. Differential size-frequency distribution of NPLD crater population is plotted in red. The Daubar et al. [5] isochrons for 0.5, 1 and 2 kyr are shown in solid black while the Hartmann [4] isochrons for 5, 10 and 20 kyr are shown in dashed blue.

We will present the results from modeling of the infilling within these small craters. DTMs will allow for detailed modeling within the interiors of craters that we can compare with observations. With these models in hand, we will use thermal models after the one described in [12] to estimate the accumulation rate of a flat surface on the current NPLD.

References: [1] Herkenhoff, K.E., Plaut J.J. 2000. *Icarus* 144: 243–53 [2] Tanaka KL. 2005. *Nature* 437:991–94 [3] Banks, M.E., et al. 2010. *JGR* 10.1029/2009JE003523 [4] Hartmann, W. K. 2005. *Icarus*, 174:294–320. [5] Daubar, I.J., et al. 2013. *Icarus* 10.1016/j.icarus.2013.04.009 [6] Sutton, S. S. et al., 2015. LPSC 46 abstract #3010. [7] Pike, R. J., 1974. *GRL* 10.1029/GL001i007p00291 [8] Phillips, R.J. et al., 2008. *Science* 10.1126/science.1157546 [9] Richardson, J.E., et al. 2007. *Icarus*, 10.1016/j.icarus.2007.08.033 [10] Sori, M.M. et al. 2015. LPSC 46 abstract #1541. [11] Gehrels, N. 1986. *ApJ*, 10.1086/164079 [12] Kieffer, H.H. 2013. *JGR* 10.1029/2012JE004164

Additional Information: This work was made possible through grant NNX13AG72G and NSF GRFP DGE-1143953. The authors also acknowledge the helpful training in DTM generation provided by S. Sutton.